www.nature.com/aps

Acta Pharmacologica Sinica

ARTICLE

A GLP-1 analog lowers ER stress and enhances protein folding to ameliorate homocysteine-induced endothelial dysfunction

Chak Kwong Cheng[1,2], Jiang-Yun Luo[1,2], Chi Wai Lau[1,2], William Chi-shing Cho[3], Chi Fai Ng[4], Ronald Ching Wan Ma[5], Xiao Yu Tian[1,2] and Yu Huang[1,2]

Hyperhomocysteinemia (HHcy) is an independent risk factor for cardiovascular diseases and increases mortality in type 2 diabetic patients. HHcy induces endoplasmic reticulum (ER) stress and oxidative stress to impair endothelial function. The glucagon-like peptide 1 (GLP-1) analog exendin-4 attenuates endothelial ER stress, but the detailed vasoprotective mechanism remains elusive. The present study investigated the beneficial effects of exendin-4 against HHcy-induced endothelial dysfunction. Exendin-4 pretreatment reversed homocysteine-induced impairment of endothelium-dependent relaxations in C57BL/6 mouse aortae ex vivo. Four weeks subcutaneous injection of exendin-4 restored the impaired endothelial function in both aortae and mesenteric arteries isolated from mice with diet-induced HHcy. Exendin-4 treatment lowered superoxide anion accumulation in the mouse aortae both ex vivo and in vivo. Exendin-4 decreased the expression of ER stress markers (e.g., ATF4, spliced XBP1, and phosphorylated eIF2α) in human umbilical vein endothelial cells (HUVECs), and this change was reversed by cotreatment with compound C (CC) (AMPK inhibitor). Exendin-4 induced phosphorylation of AMPK and endothelial nitric oxide synthase in HUVECs and arteries. Exendin-4 increased the expression of endoplasmic reticulum oxidoreductase (ERO1α), an important ER chaperone in endothelial cells, and this effect was mediated by AMPK activation. Experiments using siRNA-mediated knockdown or adenoviral overexpression revealed that ERO1α mediated the inhibitory effects of exendin-4 on ER stress and superoxide anion production, thus ameliorating HHcy-induced endothelial dysfunction. The present results demonstrate that exendin-4 reduces HHcy-induced ER stress and improves endothelial function through AMPK-dependent ERO1α upregulation in endothelial cells and arteries. AMPK activation promotes the protein folding machinery in endothelial cells to suppress ER stress.

Keywords: homocysteine; GLP-1 analog; exendin-4; AMPK; ER stress; ER chaperone; oxidative stress; endothelial dysfunction

Acta Pharmacologica Sinica (2021) 42:1598–1609; https://doi.org/10.1038/s41401-020-00589-x

INTRODUCTION

Hyperhomocysteinemia (HHcy) is an independent risk factor for cardiovascular diseases (CVDs), such as coronary heart disease and stroke [1]. A previous clinical trial reported a positive association of the serum homocysteine (Hcy) level with the incidence of coronary artery disease [2]. In addition to CVDs, HHcy is considered a risk factor for higher mortality in type 2 diabetic patients compared to nondiabetic individuals [3]. HHcy can directly induce endothelial dysfunction, one of the early indicators of atherosclerosis and vascular complications [4]. Importantly, endothelial dysfunction predisposes diabetic individuals to cardiovascular complications [5]. Another earlier clinical study also showed a positive correlation between Hcy level and cardiovascular mortality in type 2 diabetic patients [6].

Hcy induces oxidative stress and endoplasmic reticulum (ER) stress in endothelial cells; it increases the production of reactive oxygen species (ROS) by activating NADPH oxidases and xanthine oxidase, thus causing endothelial nitric oxide synthase (eNOS) uncoupling [7]. Excess ROS inactivates nitric oxide (NO), resulting in impaired endothelium-dependent NO-mediated vasodilatation, as a key index for endothelial dysfunction [8]. Furthermore, Hcy induces ER stress by modifying protein structure. As a nongenetically encoded amino acid and homolog of cysteine, Hcy can disrupt disulfide bond formation and be incorporated into proteins to posttranslationally change the protein structure [9]. Such Hcy-induced structural alteration exacerbates protein misfolding and protein aggregation, resulting in an increased burden on the refolding machinery of the ER and subsequent ER stress [10]. Elevated ER stress in endothelial cells raises oxidative stress and thus aggravates endothelial dysfunction [11].

Derived from intestinal enteroendocrine L cells, glucagon-like peptide 1 (GLP-1) is a postprandial peptide responsible for homeostasis of systemic blood glucose [12]. GLP-1 has a particularly short half-life (2 min) in vivo due to its rapid degradation mediated by dipeptidylpeptidase 4 (DPP4) and renal clearance [13]. This phenomenon has prompted the development of long-acting DPP4-resistant GLP-1 analogs, including exenatide (exendin-4), semaglutide, and liraglutide [14]. Pharmacological

[1]School of Biomedical Sciences and Li Ka Shing Institute of Health Science, The Chinese University of Hong Kong, Hong Kong SAR, China; [2]Heart and Vascular Institute and Shenzhen Research Institute, The Chinese University of Hong Kong, Hong Kong SAR, China; [3]Department of Clinical Oncology, Queen Elizabeth Hospital, Kowloon, Hong Kong SAR, China; [4]Department of Surgery, The Chinese University of Hong Kong, Hong Kong SAR, China and [5]Department of Medicine and Therapeutics, Hong Kong Institute of Diabetes and Obesity, and The Li Ka Shing Institute of Health Sciences, The Chinese University of Hong Kong, Hong Kong SAR, China
Correspondence: Xiao Yu Tian (xytian@cuhk.edu.hk) or Yu Huang (yu-huang@cuhk.edu.hk)

Received: 4 August 2020 Accepted: 15 October 2020
Published online: 25 January 2021

elevation of GLP-1 by the DPP4 inhibitor sitagliptin improved endothelium-dependent relaxations (EDRs) in the renal arteries of spontaneously hypertensive rats by activating 5′ adenosine monophosphate-activated protein kinase (AMPK) [15]. GLP-1 and GLP-1 analogs also reduced ROS production and inhibited ER stress in the cardiovascular system [16, 17]. Previous studies have shown the inhibitory effect of AMPK activation on ER stress in endothelial cells [18, 19]. Importantly, the GLP-1 analog exendin-4 can activate both the AMPK and cAMP-PKA pathways to limit lipotoxic ER stress in pancreatic β-cells by inducing the ER chaperone BiP, which actively participates in protein folding within the ER [20]. However, whether exendin-4 targets a similar or different molecule to inhibit ER stress in endothelial cells remains unclear.

In the present study, we hypothesize that the GLP-1 analog exendin-4 protects against HHcy-induced endothelial dysfunction by counteracting ER stress and oxidative stress to improve vascular function through an AMPK-dependent mechanism and that exendin-4 inhibits Hcy-induced ER stress and endothelial dysfunction by promoting protein folding capacity in endothelial cells.

MATERIALS AND METHODS

Materials and reagents

Exendin-4 (Cayman Chemical, Ann Arbor, MI, USA), semaglutide (Bachem, Bubendorf, Switzerland), and exendin9-39 (Ex9-39; Tocris, Abingdon, UK). Phenylephrine, acetylcholine (ACh), Hcy, CC, metformin (Met), tauroursodeoxycholic acid (TUDCA), H_2O_2, tunicamycin (Tm), N^G-nitro-*L*-arginine methyl ester (*L*-NAME), and sodium nitroprusside (SNP) were purchased from Sigma-Aldrich (Milwaukee, WI, USA), while tiron was purchased from Honeywell Riedel-de-Haën (Seelze, Germany).

Animal protocol

The present investigation was approved by the Animal Experimentation Ethics Committee, Chinese University of Hong Kong (CUHK). All experiments were in accordance with the Guide for the Care and Use of Laboratory Animals issued by the National Institutes of Health. Animal studies are reported in compliance with the ARRIVE guidelines [21]. Male C57BL/6 mice (8 weeks old, 22–25 g) were provided by the CUHK Laboratory Animal Services Center. Male C57BL/6 mice were fed a normal chow (control) or high methionine low folate (HMLF) diet (20 $g \cdot kg^{-1}$ *L*-methionine, 0.0015 $g \cdot kg^{-1}$ folic acid, TD.98272; Envigo Teklad, Madison, WI, USA) for 12 weeks to develop diet-induced HHcy. The body weights of the mice were recorded. The mice were later subcutaneously injected with vehicle (saline) or exendin-4 (40 $\mu g \cdot kg^{-1}$) suspended in saline every other day for 4 weeks. All mice were housed at constant temperature (23 ± 1 °C) and humidity (55% ± 5%) under a 12 h light:12 h dark cycle in individually well-ventilated caging systems with free access to laboratory food pellets and water. The mice were randomly divided into four groups: normal chow (control), HMLF diet, exendin-4, and exendin-4 + HMLF diet.

Blood glucose measurement

After 12 weeks of the HMLF diet, a glucose tolerance test and insulin tolerance test were performed on the mice after 6 h of fasting. Upon intraperitoneal injection of either glucose (1 $g \cdot kg^{-1}$) or insulin (1 unit $\cdot kg^{-1}$), the glucose levels were measured in venous blood from the mouse tail at 0, 15, 30, 60, 90, and 120 min.

Ex vivo organ culture of mouse aortic rings

After mice were sacrificed by CO_2 suffocation, thoracic aortae were dissected out, and adhering connective tissue was removed in sterile phosphate-buffered saline (PBS). The aortae were cut into ring segments of ~2 mm in length and cultured in Dulbecco's modified Eagle's medium (DMEM; Life Technologies) containing 10% fetal bovine serum (FBS, Gibco), 100 $\mu g \cdot mL^{-1}$ streptomycin and 100 IU $\cdot mL^{-1}$ penicillin. For pharmacological experiments, some aortic rings were coincubated with Hcy (300 $\mu mol \cdot L^{-1}$, 2 h), exendin-4 (10 $nmol \cdot L^{-1}$, 4 h), semaglutide (10 $nmol \cdot L^{-1}$, 4 h), the GLP-1 receptor (GLP-1R) antagonist Ex9-39 (100 $nmol \cdot L^{-1}$, 5 h), the AMPK inhibitor CC (10 $\mu mol \cdot L^{-1}$, 5 h), Met (100 $\mu mol \cdot L^{-1}$, 4 h), the ROS scavenger tiron (1 $mmol \cdot L^{-1}$, 4 h), the ER stress alleviator TUDCA (10 $\mu mol \cdot L^{-1}$, 4 h), the ER stress inducer Tm (1 $\mu g \cdot mL^{-1}$, 2 h), or H_2O_2 (1 $mmol \cdot L^{-1}$, 2 h) (Fig. 1a). For ex vivo adenoviral transduction, rings were infected with Ad-vector or Ad-CMV-ERO1α (Vigene Biosciences, Rockville, MD, USA) for 12 h prior to functional assays on a myograph. After incubation, the rings were transferred to chambers filled with Krebs–Henseleit solution containing ($mmol \cdot L^{-1}$) 119 NaCl, 4.7 KCl, 1 $MgCl_2$, 2.5 $CaCl_2$, 1.2 KH_2PO_4, 25 $NaHCO_3$, and 11 D-glucose and subsequently mounted on a myograph for measurement of isometric tension. In addition, some rings were used for detection of superoxide anion production by dihydroethidium (DHE) staining or by lucigenin-enhanced chemiluminescence.

Functional assay by wire myography

The thoracic aortae and mesenteric arteries (second order) were cut into ring segments of ~2 mm in length in ice-cold and oxygenated Krebs solution and then mounted individually on the Multi Wire Myograph System (Danish Myo Technology, Aarhus, Denmark) for functional assays. Each ring was initially stretched to an optimal baseline tension (3 mN for aortae and 2 mN for mesenteric arteries) and allowed to equilibrate for 1 h under continuous oxygenation (95% O_2, 5% CO_2) at 37 °C in Krebs solution. The rings were precontracted with 60 $mmol \cdot L^{-1}$ KCl and then rinsed three times in Krebs solution. Subsequently, phenylephrine (3 $\mu mol \cdot L^{-1}$) was added to precontract the rings, and EDRs were induced by cumulative additions of ACh (3 $nmol \cdot L^{-1}$ to 10 $\mu mol \cdot L^{-1}$) [22]. Prior to EDRs, some mesenteric arteries were pretreated with the NOS inhibitor *L*-NAME (100 $\mu mol \cdot L^{-1}$, 30 min). Endothelium-independent relaxation was also determined by cumulative additions of SNP (1 $nmol \cdot L^{-1}$ to 10 $\mu mol \cdot L^{-1}$) into the bathing solution. Changes in isometric tension were monitored by the PowerLab LabChart 7.0 system (AD Instruments, Bella Vista, NSW, Australia).

Plasma Hcy determination by ELISA

Mouse blood was collected by cardiac puncture in the presence of heparin. The blood was centrifuged for 10 min at 1000 × *g* at 4 °C to obtain plasma. The plasma Hcy level was determined by an ELISA kit (Cell Biolabs, San Diego, CA, USA) according to the manufacturer's protocol.

Culture of human umbilical vein endothelial cells (HUVECs)

HUVECs (Lonza, Walkersville, MD, USA, Cat# CC-2519) were cultured in endothelial cell growth medium (EGM; Lonza) supplemented with 10% FBS and antibiotics until confluency. Cells at passages four to seven were used for the experiments. For adenoviral infection, HUVECs were transfected with Ad-vector or Ad-CMV-ERO1α (Vigene Biosciences) in FBS-free DMEM for 4 h before incubation in EGM for 20 h. For pharmacological experiments, HUVECs were pretreated with Hcy (300 $\mu mol \cdot L^{-1}$, 4 h), exendin-4 (10 $nmol \cdot L^{-1}$, 8 h), semaglutide (10 $nmol \cdot L^{-1}$, 8 h), Ex9-39 (100 $nmol \cdot L^{-1}$, 10 h), or CC (10 $\mu mol \cdot L^{-1}$, 10 h) prior to ROS detection, RT-PCR, and Western blotting.

Small interfering RNA (siRNA)-mediated genetic knockdown
After reaching 80% confluency, HUVECs were transfected with scrambled siRNA (Invitrogen) or siRNA targeting ER oxidoreductase 1α (ERO1α) (siERO1α; Invitrogen) through electroporation by an Amaxa Basic Nucleofector Kit specialized for mammalian endothelial cells (Lonza) [23]. In brief, HUVECs were trypsinized and washed twice in PBS. The cells were resuspended in 100 μL of basic nucleofector solution and then transferred to an electroporation vial containing either 50 pmol scrambled siRNA or siERO1α. The cells were electroporated by an Amaxa Nucleofector™ apparatus and plated in six-well plates containing FBS-free DMEM. The medium was changed to EGM after 12 h, and the cells were exposed to exendin-4 (10 nmol · L^{-1}, 8 h) and/or Hcy (300 μmol · L^{-1}, 4 h) before ROS measurement and Western blotting.

ROS measurement by DHE staining
As previously described [24], ROS production in the *en face* endothelium of the mouse aortae and HUVECs was detected by DHE fluorescence. Some aortic rings were frozen within optimal cutting temperature compound (Sakura Finetek, Flemingweg, Holland) and then sliced into 10 μm sections by a Leica CM 1000 cryostat (Leica Biosystems, Wetzlar, Germany). Briefly, freshly isolated aortic rings, frozen aortic cross sections and HUVECs were incubated with DHE (5 μmol · L^{-1}; Invitrogen) in normal physiological saline solution (NPSS, in mmol · L^{-1}: 140 NaCl, 5 KCl, 1 $MgCl_2$, 1 $CaCl_2$, 5 HEPES and 10 glucose, pH 7.4). Subsequently, the tissues and cells were rinsed three times in NPSS. The aortic rings were longitudinally cut open to expose the *en face* endothelium. Fluorescence images were taken by an Olympus Fluoview FV1000 laser scanning confocal system (Olympus, Japan) (DHE: excitation: 515 nm, emission: 585 nm; elastin autofluorescence: excitation: 488 nm, emission: 520–535 nm). DHE fluorescence is presented in real numbers.

Superoxide anion detection by lucigenin-enhanced chemiluminescence assay
The amount of superoxide anion in mouse aortae was measured using the lucigenin-enhanced chemiluminescence method [25]. Briefly, dissected mouse aortae were preincubated in Krebs-HEPES solution (in mmol · L^{-1}: 99 NaCl, 25 $NaHCO_3$, 4.7 KCl, 1.2 $MgSO_4$, 2.5 $CaCl_2$, 1 KH_2PO_4, 11 glucose, and 20 Na-HEPES, pH 7.4), supplemented with 1 mmol · L^{-1} diethyldithiocarbamic acid (Sigma-Aldrich) and 0.1 mmol · L^{-1} β-NADPH (Sigma-Aldrich) at 37 °C for 45 min. The aortae were thereafter transferred to vials containing Krebs-HEPES solution in the presence of 10 μmol · L^{-1} lucigenin (Sigma-Aldrich). Repeated measurements were recorded by a GloMax® 20/20 Luminometer (Madison, WI, USA) for 10 min in 1-min intervals. Superoxide anion production was presented in real numbers in relative light units per milligram of dry tissue.

Quantitative RT-PCR
Total RNA from HUVECs was extracted with TRIzol reagent (Invitrogen). cDNA was synthesized using the iScript™ cDNA synthesis kit (Bio-Rad). Quantitative RT-PCR was performed by SYBR Premix Ex Taq (Takara, Shiga Prefecture, Kusatsu, Japan) in an ABI ViiA7 system (Applied Biosystems, Waltham, MA, USA). GAPDH served as an endogenous control. Gene expression was quantified by the comparative C(t) (ΔΔCt) method and expressed compared with the control. The primer pairs for ATF4 were 5′-AA ACCTCATGGGTTCTCCAG-3′ (forward) and 5′-GGCATGGTTTCCAGG TCATC-3′ (reverse); the primer pairs for ATF6 were 5′-AATTCTCAG CTGATGGCTGT-3′ (forward) and 5′-TGGAGGATCCTGGTGTCCAT-3′ (reverse); the primer pairs for spliced XBP1 were 5′-TGCTGAGTCCG CAGCAGGTG-3′ (forward) and 5′-GCTGGCAGGCTCTGGGGAAG-3′ (reverse); and the primer pairs for GAPDH were 5′-GAAGGTGAAG GTCGGAGTC-3′ (forward) and 5′-GAAGATGGTGATGGGATTTC-3′ (reverse). The expression of mRNAs was normalized to the mean of the untreated control and is expressed as the relative fold change as a standard practice for RT-PCR data. Untreated control samples retained their individual fold change.

Western blotting
HUVECs and mouse aortae were homogenized in ice-cold 1X RIPA lysis buffer supplemented with phosSTOP phosphatase inhibitor (Roche, Basel, Switzerland) and a cOmplete Protease Inhibitor Cocktail (Sigma-Aldrich). The protein concentration was determined by a BCA protein assay kit (Pierce Biotechnology, Rockford, USA). Twenty micrograms of protein samples was resolved by a 10% SDS-polyacrylamide gel and transferred onto an Immobilon-P polyvinylidene difluoride membrane (Millipore Corp., Bedford, MA, USA). Nonspecific binding sites were blocked by 3% BSA containing 0.05% Tween-20 TBS. The blots were incubated at 4 °C overnight with primary antibodies: anti-phospho-AMPKα at Thr172 (1:1000; Cell Signaling Technology, Cat# 2531S), anti-AMPKα (1:1000; Cell Signaling Technology, Cat# 2532S), anti-phospho-eNOS at Ser1177 (1:1000; Cell Signaling Technology, Cat# 9571S), anti-eNOS (1:1000; BD Transduction Laboratory, San Diego, CA, USA, Cat# 610297), anti-phospho-eIF2α (1:1000; Invitrogen, Cat# 44-728G), anti-eIF2α (1:1000; Cell Signaling Technology, Cat# 9722S), anti-ERO1α (1:1000; Invitrogen, Cat# PA5-29535), and anti-GAPDH (1:10000, Cell Signaling Technology, Cat# 2118S). Bound antibodies were incubated with horseradish peroxidase-conjugated secondary antibody (Cell Signaling Technology) at room temperature for 1 h and were later visualized by the enhanced chemiluminescence detection system (Cell Signaling Technology). Quantification was performed by ImageJ free software (Version 1.47). Each lane was normalized to GAPDH.

Experimental blinding and randomization
Experimental blinding was undertaken to lower the risk of bias in this investigation whenever possible. The drugs used for the in vitro, ex vivo, and in vivo experiments were prepared by laboratory members who did not perform the experiments. Furthermore, all animals were randomized prior to treatments. The results were acquired from a group with a size of at least five for all experimental protocols and data analyses in this study.

Statistical analysis
The results represent the mean ± SEM of *n* experiments. Statistical analyses were performed using GraphPad Prism software (Version 6.0). Statistical significance was determined by one-way ANOVA followed by Tukey's multiple comparisons test for comparison of more than two groups. P value < 0.05 indicates statistical significance.

RESULTS

Exendin-4 ex vivo rescued Hcy-induced endothelial dysfunction in mouse aortae
The protocol for the functional assay of isolated mouse aortae is shown in Fig. 1a. Treatment with Hcy at 300 μmol · L^{-1} for 2 h markedly impaired ACh-induced EDRs in aortae (Fig. 1b). Preincubation with 10 nmol · L^{-1} of the GLP-1 analogs exendin-4 or semaglutide prior to the addition of Hcy reversed the reduced EDRs (Fig. 1b, c). Moreover, pretreatment with Met (an antidiabetic drug and AMPK activator; 100 μmol · L^{-1}), tiron (an ROS scavenger; 1 mmol · L^{-1}), or TUDCA (an ER stress alleviator; 10 μmol · L^{-1}) also improved EDRs in the Hcy-treated aortae (Fig. 1d). The effect of exendin-4 and semaglutide on EDRs was antagonized by Ex9-39 (a GLP-1 receptor antagonist; 100 nmol · L^{-1}) and CC (an AMPK inhibitor; 10 μmol · L^{-1}) (Fig. 1c). Hcy did not alter SNP-induced endothelium-independent relaxations (Supplementary Information, Fig. S1).

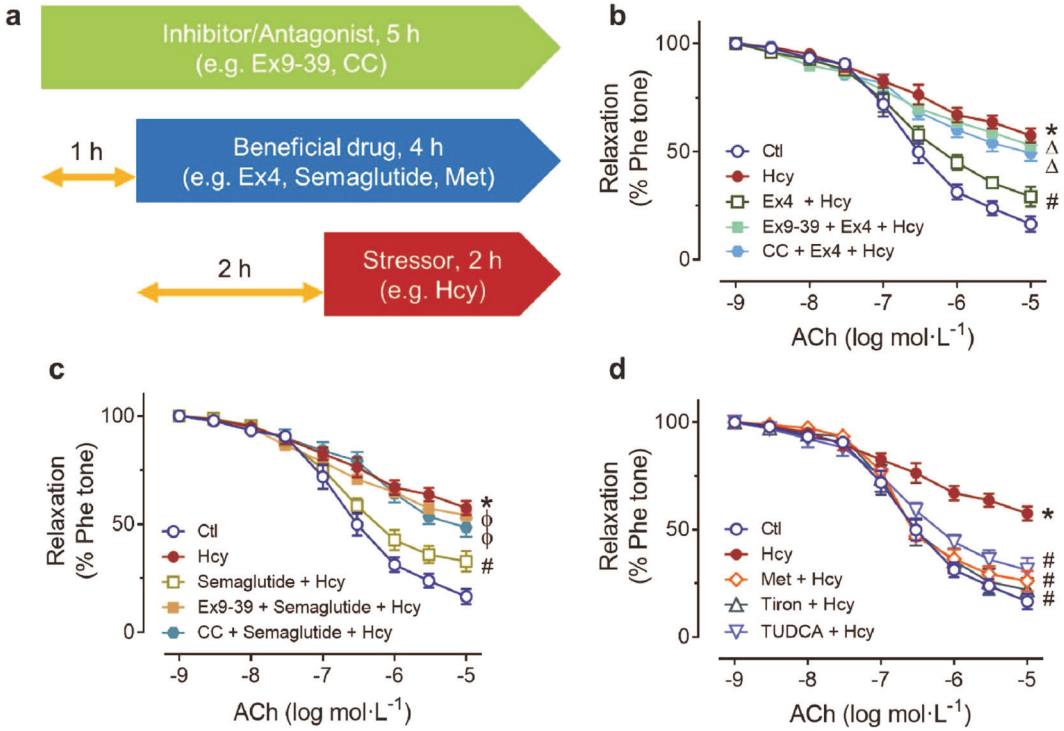

Fig. 1 Vascular function of mouse aortae upon acute Hcy exposure. a Protocol for the pharmacological treatment of isolated mouse aortae. **b** Ex vivo Ex4 treatment restored Hcy-induced endothelial dysfunction via AMPK activation. **c** Ex vivo treatment with another GLP-1 analog, semaglutide, also reversed Hcy-impaired endothelial function. **d** Acute treatment of different drugs that improved EDRs of Hcy-incubated mouse aortae. The same curves for the Ctl and Hcy groups in **b**–**d**. $^{*}P < 0.05$ vs the Ctl group; $^{\#}P < 0.05$ vs the Hcy group; $^{\Delta}P < 0.05$ vs the Ex4 + Hcy group. $^{\Phi}P < 0.05$ vs the semaglutide + Hcy group. CC compound C, Ex4 exendin-4, Ex9-39 exendin9-39, Hcy homocysteine, Met metformin, TUDCA tauroursodeoxycholic acid. The data are the mean ± SEM ($n = 6$–7 per group).

Exendin-4 in vivo improved endothelial function of both conduits and small arteries from the mice with diet-induced HHcy

A 12-week HMLF diet increased the plasma level of Hcy in C57BL/6 mice from ~80 to ~200 $\mu mol \cdot L^{-1}$ (Fig. 2a). The HMLF diet and exendin-4 slightly decreased the body weight of C57BL/6 mice (Supplementary Information, Fig. S2a). The HMLF diet-induced mild glucose intolerance in the mice (Supplementary Information, Fig. S2b, c) without changing the insulin sensitivity (Supplementary Information, Fig. S2d, e). In contrast, chronic exendin-4 treatment improved glucose tolerance (Supplementary Information, Fig. S2b, c) in the C57BL/6 mice. EDRs in the aortae (Fig. 2b) and mesenteric arteries (Fig. 2c) from the mice with HHcy were diminished compared to those in the control mice. Subcutaneous injection of exendin-4 restored the impaired EDRs in both aortae (Fig. 2b) and mesenteric arteries (Fig. 2d) in the mice with HHcy. The HMLF diet and chronic exendin-4 treatment did not affect endothelium-independent aortic relaxations (Supplementary Information, Fig. S3). Importantly, *L*-NAME treatment to inhibit NO production reduced EDRs and eliminated the differences in concentration–response curves of the mesenteric arteries in response to ACh in all groups (Fig. 2c–e), suggesting that the improved EDRs after exendin-4 treatment are most likely due to preserved NO bioavailability.

Exendin-4 ex vivo and in vivo lowered Hcy-induced superoxide generation in the mouse aortae

Both 2-h acute Hcy treatment (300 $\mu mol \cdot L^{-1}$) ex vivo and chronic HMLF diet feeding (12 weeks) increased the level of ROS (mainly superoxide anions) in the mouse aortae as measured by DHE staining (Fig. 3a–e) and lucigenin-enhanced chemiluminescence (Fig. 3c, f). In contrast, acute exendin-4 coculture (10 $nmol \cdot L^{-1}$) and chronic exendin-4 subcutaneous injection (40 $\mu g \cdot kg^{-1}$, on alternative days, 4 weeks) normalized superoxide anion overproduction in the mouse aortae (Fig. 3). Ex vivo exposure to semaglutide (10 $nmol \cdot L^{-1}$) or tiron (1 $mmol \cdot L^{-1}$) also inhibited Hcy-induced ROS generation in the *en face* endothelium of the mouse aortae (Fig. 3a–c). Similar to the vascular functional results, the inhibitory effects of exendin-4 or semaglutide on ROS overproduction were reversed by the GLP-1 receptor antagonist Ex9-39 (100 $nmol \cdot L^{-1}$) (Fig. 3a–c). H_2O_2 (1 $mmol \cdot L^{-1}$) was used as a positive control to directly increase ROS (Fig. 3a–c).

GLP-1 analogs restored the reduced phosphorylation of AMPK and eNOS in Hcy-treated endothelial cells

Acute treatment with Hcy (300 $\mu mol \cdot L^{-1}$) reduced the phosphorylation of both AMPKα (p-AMPKα; Fig. 4a, c, d, f) and eNOS (p-eNOS; Fig. 4a, b, d, e) in HUVECs, and this effect was reversed by 8-h treatment with either exendin-4 (10 $nmol \cdot L^{-1}$) or semaglutide (10 $nmol \cdot L^{-1}$). Likewise, HMLF diet feeding also reduced the levels of both p-AMPKα and p-eNOS in the mouse aortae, which was reversed by chronic exendin-4 treatment (Fig. 4g–i).

Exendin-4 suppressed ER stress and ER stress-induced ROS generation in Hcy-treated endothelial cells

Ex vivo treatment with exendin-4 attenuated ER stress-induced ROS production as measured by DHE staining and lucigenin-enhanced chemiluminescence (Fig. 5a–c). Exposure to either the ER stress inducer Tm (1 $\mu g \cdot mL^{-1}$) or Hcy (300 $\mu mol \cdot L^{-1}$) for 2 h induced ROS elevation in the *en face* endothelium of the mouse aortae, which was inhibited by pretreatment with

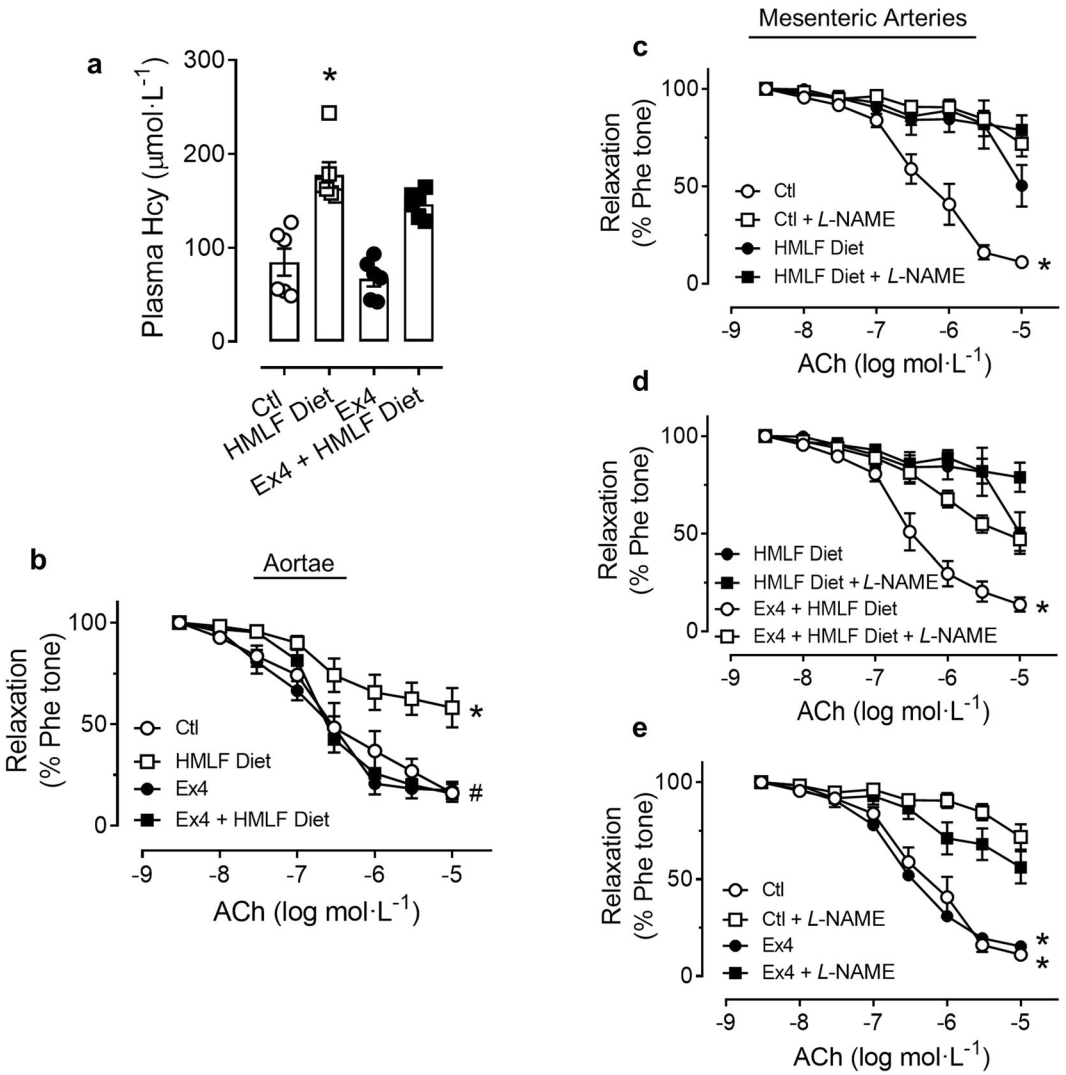

Fig. 2 Vascular function of the conduit and small arteries of the mice with diet-induced HHcy. a The HMLF diet elevated plasma Hcy levels in C57BL/6 mice. **b** Chronic treatment with Ex4 restored EDRs in aortae from the mice with diet-induced HHcy. $^{*}P < 0.05$ vs the Ctl group; $^{\#}P < 0.05$ vs the HMLF diet group. **c**–**e** EDRs in the mesenteric arteries (second branch) with or without *L*-NAME in all groups of **b**. Same Ctl and Ctl + *L*-NAME curves for **c** and **e**. Same HMLF diet and HMLF diet + *L*-NAME curves for **c** and **d**. $^{*}P < 0.05$ vs *L*-NAME. Ex4 exendin-4, HMLF high methionine low folate, *L*-NAME N^{G}-nitro-*L*-arginine methyl ester. The data are presented as the mean ± SEM ($n = 6$ per group).

exendin-4 (10 nmol · L^{-1}) or the ER stress alleviator TUDCA (10 μmol · L^{-1}), indicating that Hcy-induced ROS elevation depends on increased ER stress. In contrast, H_2O_2-triggered ROS production was not affected by TUDCA, further supporting the critical role of ER stress in Hcy-induced ROS elevation. Moreover, AMPK inhibition by CC reversed the inhibitory effect of exendin-4 on ROS elevation (Fig. 5a–c), indicating that AMPK activation is likely to mediate the effect of exendin-4. Both RT-PCR and Western blotting results showed that exendin-4 reversed the increased expression of the ER stress markers ATF6, spliced XBP1, ATF4, and p-eIF2α (three arms of the ER stress pathway) in the Hcy-treated HUVECs (Fig. 6a–e). This ER stress-inhibiting benefit of exendin-4 was abolished by Ex9-39 or CC (Fig. 6a–e). In the aortae of the mice with diet-induced HHcy, chronic exendin-4 treatment suppressed the expression of the ER stress marker p-eIF2α (Fig. 6g, h). Taken together, these results indicate that exendin-4 activates AMPK to inhibit Hcy-induced ER stress which associates with ROS elevation in endothelial cells.

Exendin-4 inhibited Hcy-induced ER stress by promoting protein folding capacity

To further identify the target of GLP-1 receptor activation to reduce ER stress, we found that the expression of ERO1α, an important ER chaperone, was reduced both in the Hcy-treated HUVECs and in the aortae of the mice with diet-induced HHcy, and was reversed by exendin-4 treatment (Fig. 6d, f, g, i). In HUVECs, the exendin-4-induced increase in ERO1α protein was reversed by cotreatment with Ex9-39 or CC (Fig. 6d, f). Furthermore, ERO1α knockdown by siERO1α (Fig. 7a, b) reversed the inhibitory effect of exendin-4 on the Hcy-induced elevation of p-eIF2α (Fig. 7a, d) without affecting exendin-4-induced eNOS phosphorylation (Fig. 7a, c). However, the ROS-lowering effect of exendin-4 in the Hcy-treated HUVECs (Fig. 7e, f) was attenuated by siERO1α, implying that exendin-4 upregulates ERO1α to inhibit ER stress-induced ROS elevation, while eNOS activation might be mediated by other mechanisms.

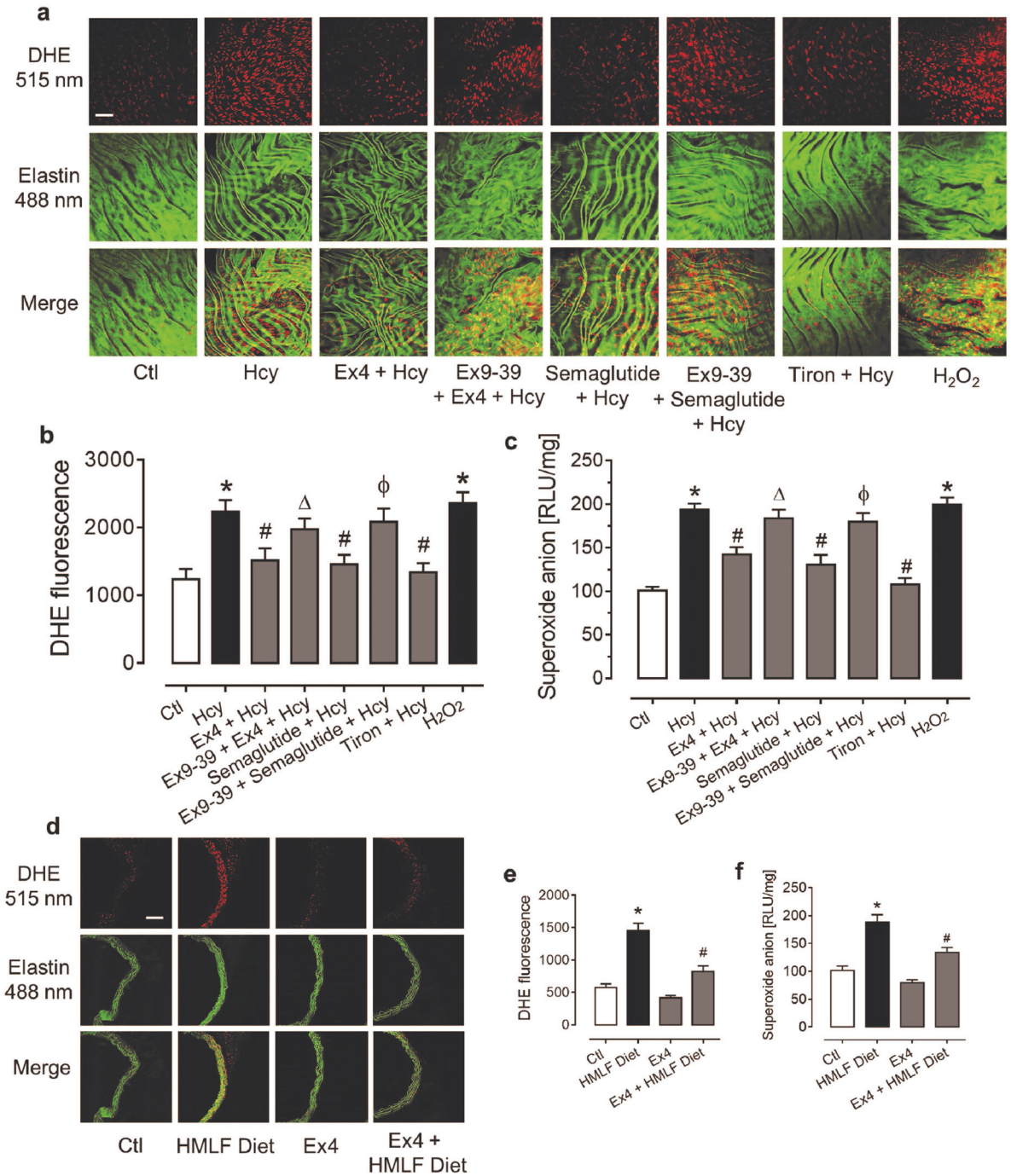

Fig. 3 ROS level of mouse aortae ex vivo and in vivo. a Representative images of DHE staining (x500) in the *en face* endothelium of mouse aortae upon acute pharmacological treatments. Ex vivo incubation of GLP-1 analogs, Ex4 and semaglutide, suppressed Hcy-induced oxidative stress, as revealed by **b** DHE staining and **c** lucigenin-enhanced chemiluminescence assay. $^{*}P < 0.05$ vs the Ctl group; $^{\#}P < 0.05$ vs the Hcy group; $^{\Delta}P < 0.05$ vs the Ex4 + Hcy group. $^{\Phi}P < 0.05$ vs the semaglutide + Hcy group. $n = 6$ per group. **d** Representative images of DHE staining (x500) in cross sections of aortae from the mice with diet-induced HHcy. Chronic treatment with Ex4 reduced ROS levels in aortae from the mice with diet-induced HHcy, as shown by **e** DHE staining and **f** lucigenin-enhanced chemiluminescence assays. $^{*}P < 0.05$ vs the Ctl group; $^{\#}P < 0.05$ vs the HMLF diet group. $n = 6$ per group. DHE dihydroethidium, Ex4 exendin-4, Ex9-39 exendin9-39, Hcy homocysteine, HMLF high methionine low folate. The data are the mean ± SEM.

ERO1α overexpression improved endothelial function by inhibiting ER stress

The above results clearly indicate that ERO1α serves as a target of GLP-1 receptor activation in endothelial cells, and we wondered whether upregulating ERO1α is vasoprotective. Indeed, overexpression of ERO1α by Ad-CMV-ERO1L (Fig. 8a, b) protected HUVECs against the Hcy-induced increase in p-eIF2α (Fig. 8a, e) and attenuated the Hcy-induced superoxide anion production (Fig. 8f, g). However, ERO1α overexpression did not affect the phosphorylation of AMPK and eNOS in HUVECs

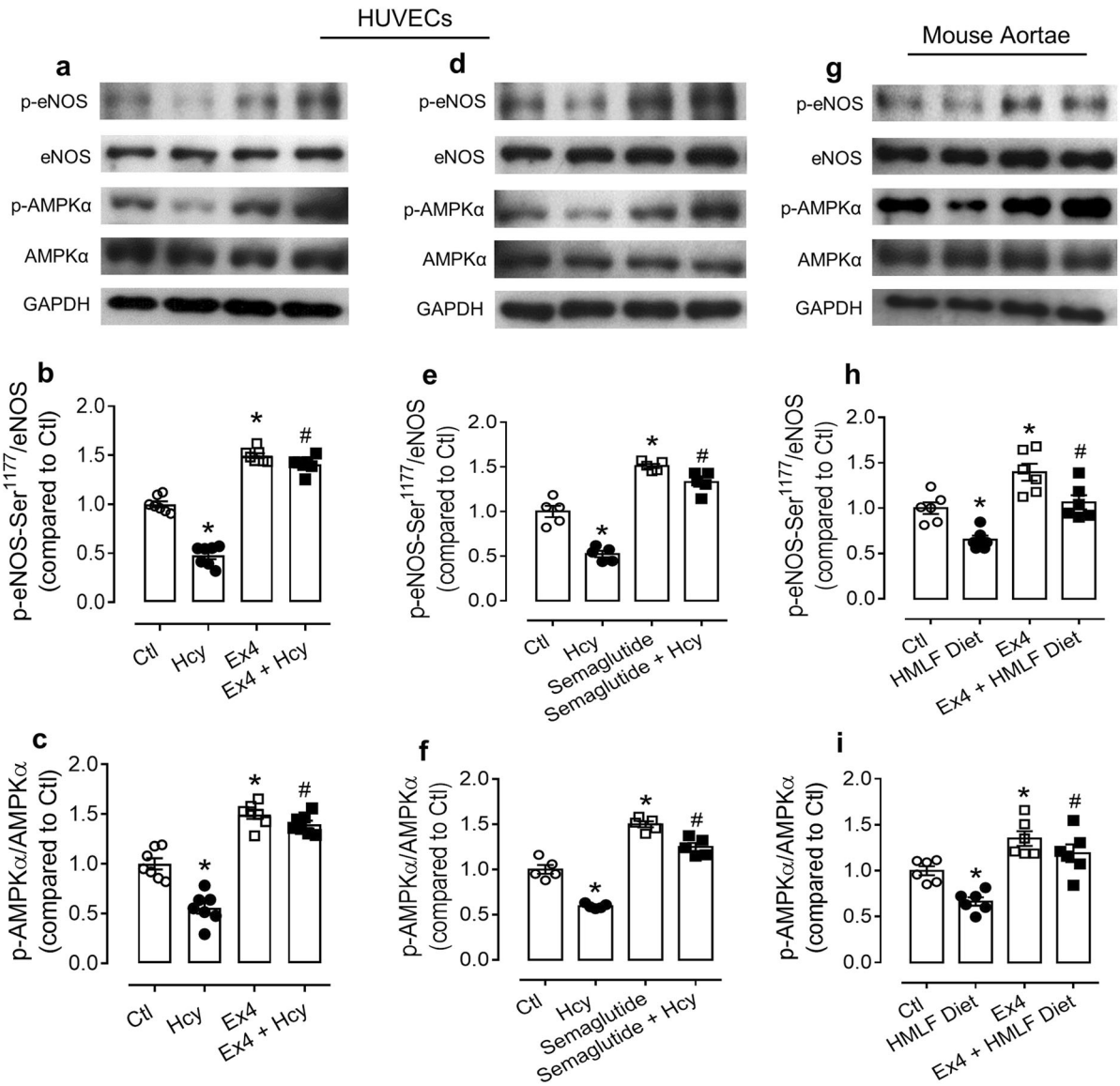

Fig. 4 Ex4-activated AMPK and eNOS in HUVECs and aortae from the mice with diet-induced HHcy. a–c Ex4 reversed HHcy-lowered expression of p-AMPKα and p-eNOS in HUVECs. **d–f** Semaglutide promoted the activation of AMPK and eNOS in the Hcy-treated HUVECs. $^{*}P < 0.05$ vs the Ctl group; $^{\#}P < 0.05$ vs the Hcy group. $n = 5–7$ per group. **g–i** Chronic Ex4 treatment upregulated the expression of both p-AMPKα and p-eNOS in the aortae of the mice with diet-induced HHcy. $^{*}P < 0.05$ vs the Ctl group; $^{\#}P < 0.05$ vs the HMLF diet group. $n = 6$ per group. Ex4 exendin-4, Hcy homocysteine, HMLF high methionine low folate. The data are presented as the mean ± SEM.

(Fig. 8a, c, d). More importantly, ERO1α overexpression in mouse aortae prior to Hcy exposure alleviated endothelial dysfunction ex vivo (Fig. 8h) without affecting endothelium-independent relaxations (Supplementary Information, Fig. S4). Taken together, the present results from gain and loss of function studies suggest that ERO1α is most likely to mediate the effect of GLP-1 receptor activation to inhibit Hcy-induced ER stress, and ERO1α functions as a downstream target of GLP-1-induced AMPK activation in protecting endothelial function in pathological situations such as HHcy.

DISCUSSION

The present study demonstrates the vascular benefit of exendin-4 in counteracting ER stress-induced endothelial dysfunction in Hcy-treated human endothelial cells and mouse isolated arteries, as well as in mice with diet-induced HHcy. The study revealed that the GLP-1 analog activates AMPK, which upregulates ERO1α to inhibit Hcy-induced ER stress and downstream ROS production, while it also increases eNOS activity that is impaired by Hcy, contributing to increased NO bioavailability. Thus, endothelial function is preserved against HHcy.

As a risk factor for CVDs in diabetic patients, Hcy induces ROS production via multiple mechanisms. Hcy can directly trigger oxidative stress by upregulating and downregulating the expression of NADPH oxidase and thioredoxin, respectively [26]. However, Hcy can also indirectly increase oxidative stress by increasing ER stress. Through posttranslational modification of proteins, Hcy causes the accumulation of misfolded proteins in the ER [10]. In our model, exendin-4 reversed ROS production likely induced by an indirect effect of Hcy through generation of ER stress in endothelial cells.

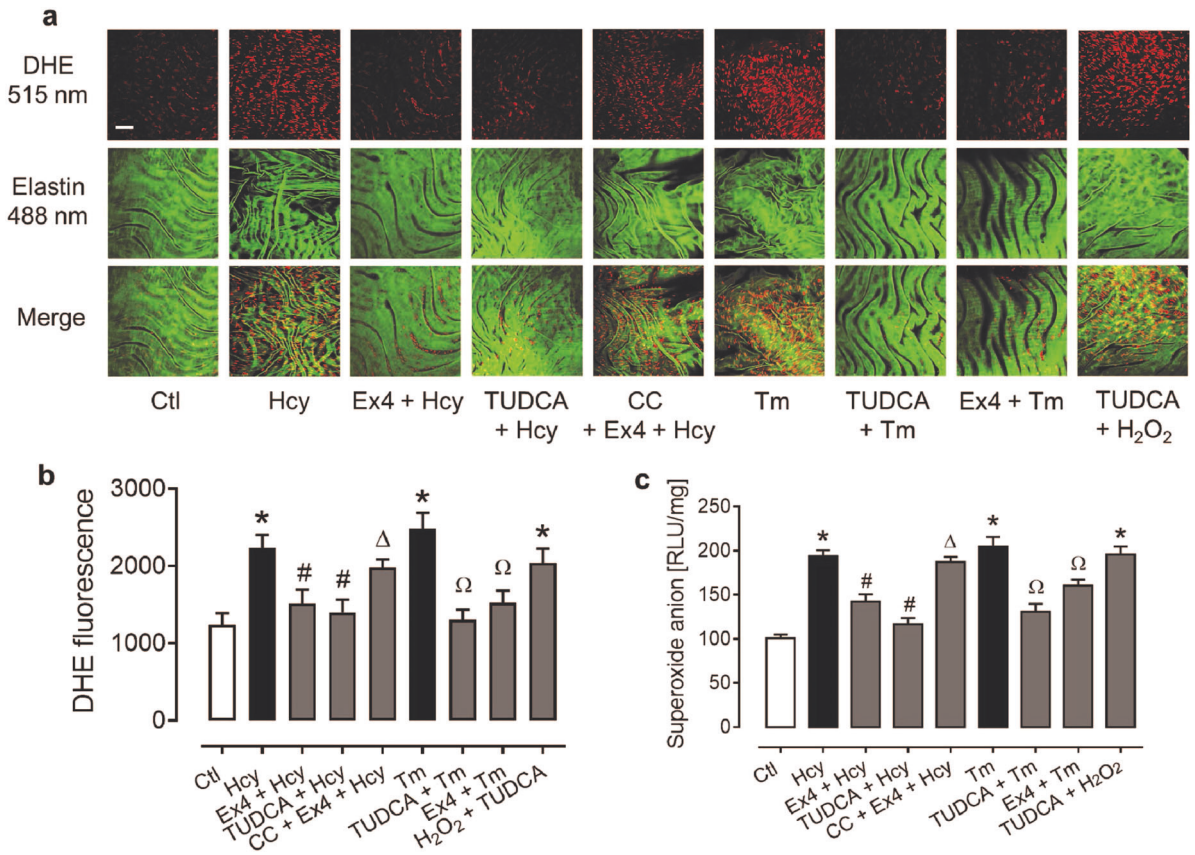

Fig. 5 ER stress-induced oxidative stress in endothelial cells. a Representative images of DHE staining (x500) in the *en face* endothelium of mouse aortae upon different pharmacological treatments. Ex vivo incubation with Ex4 lowered ER stress-induced superoxide production by AMPK activation, as revealed by **b** DHE staining and **c** lucigenin-enhanced chemiluminescence assay. $^{*}P < 0.05$ vs the Ctl group; $^{\#}P < 0.05$ vs the Hcy group; $^{\Delta}P < 0.05$ vs the Ex4 + Hcy group; $^{\Omega}P < 0.05$ vs the Tm group. $n = 6$ per group. CC compound C, DHE dihydroethidium, Ex4 exendin-4, Ex9-39 exendin9-39, Hcy homocysteine, Tm tunicamycin, TUDCA tauroursodeoxycholic acid. The data are presented as the mean ± SEM.

We and others previously showed that endothelial cells express GLP-1 receptor and the GLP-1 analogs exenatide or exendin-4 bind to GLP-1 receptor to activate AMPK [8, 27]. In the present study, the GLP-1 analogs exendin-4 and semaglutide both increased AMPK phosphorylation. As a known target of AMPK, eNOS phosphorylation was enhanced by exendin-4-induced AMPK activation. Activated eNOS is responsible for the elevated production of NO, which directly boosts EDRs [28]. The present results are consistent with a previous study by our group showing that exendin-4 and the DPP4 inhibitor sitagliptin lower oxidative stress to alleviate endothelial dysfunction in the context of hypertension [29].

The present study provides the first line of evidence that exendin-4 suppresses Hcy-induced ER stress by promoting protein folding capacity via ERO1α, an important ER chaperone. The GLP-1 analog increases the expression of this ER chaperone in endothelial cells. Although GLP-1 analogs were previously shown to inhibit ER stress in diabetic patients [17], the detailed mechanism remains partially understood. One previous study showed that GLP-1 analogs can increase the expression of another ER chaperone, BiP, in rat pancreatic β-cells [20]. Here, we demonstrated that exendin-4 elevated the expression of ERO1α through AMPK activation in endothelial cells because this effect was reversed by an AMPK inhibitor. The experiments with both ERO1α knockdown and overexpression further indicated that exendin-4-induced ERO1α expression is most likely to account for its inhibition of ER stress and subsequent ROS overproduction in endothelial cells, together suggesting ERO1α as a novel target of GLP-1 receptor activation.

ERO1α is a chaperone protein responsible for promoting protein folding of misfolded proteins in the ER [30]. ERO1α and protein disulfide isomerases cooperate to mediate the formation of proper disulfide bonds and cleavage of improper disulfide bonds in unfolded and misfolded proteins [31, 32]. This process limits the accumulation of misfolded proteins and the burden on the ER. For instance, ERO1α is crucial in improving the folding of mutant proinsulin in pancreatic β-cells to restrain ER stress [33]. Hcy is known to cause posttranslational modifications, including the formation of undesired disulfide bonds [9]. Therefore, the present study provides novel evidence that ERO1α upregulation might facilitate the cleavage of misfolded proteins and the formation of appropriate disulfide bonds to counteract HHcy-induced ER stress.

AMPK activation appears to be an important step in initiating the downstream cascade toward lowering ER stress. The present study, for the first time, shows that AMPK activation upregulates the ER chaperone ERO1α to activate the protein folding machinery in endothelial cells. The present results showed that the protein folding capacity via ERO1α was enhanced by AMPK activation, but ERO1α overexpression did

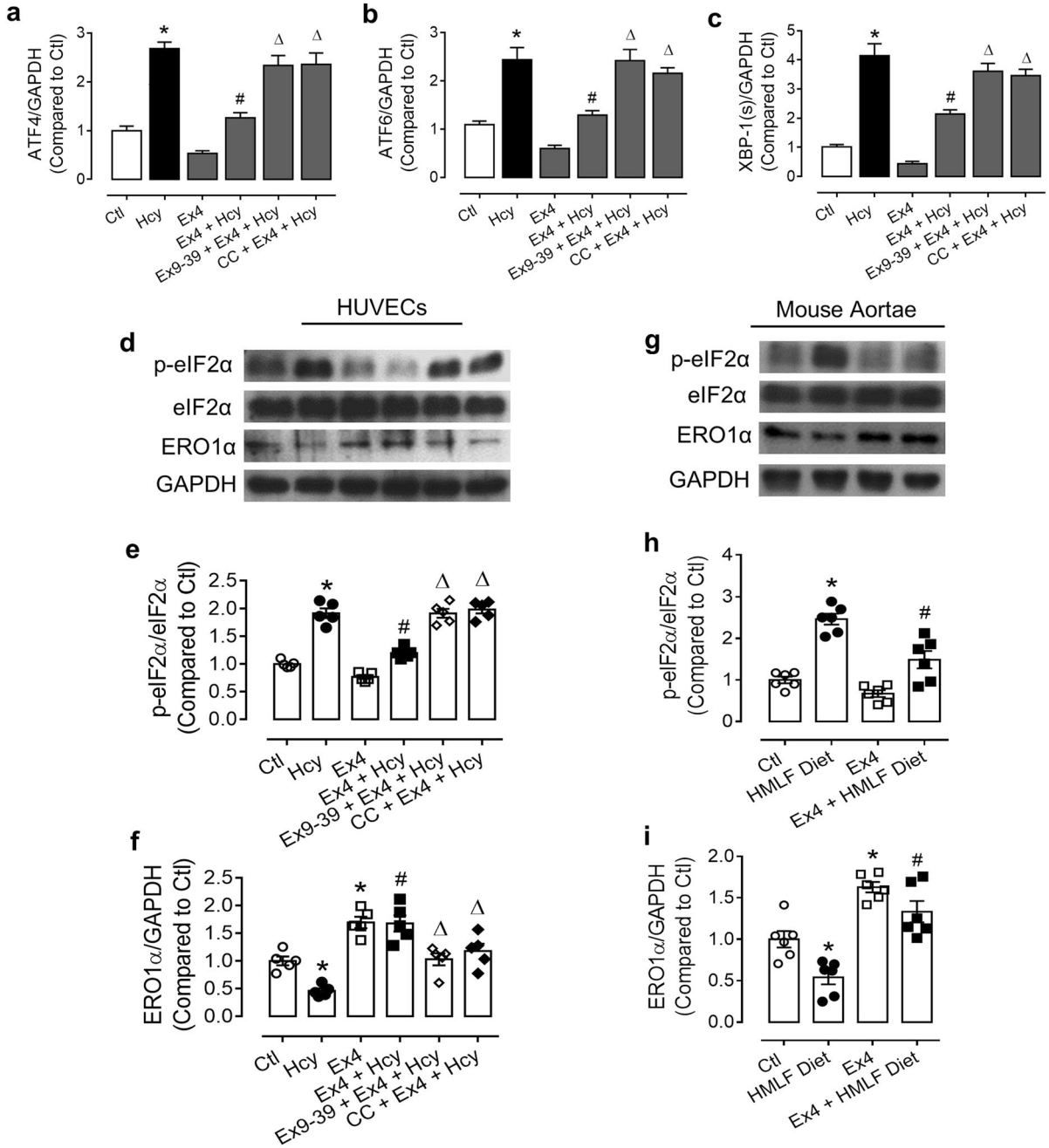

Fig. 6 ER stress and ER chaperone of endothelial cells. Coincubation of HUVECs with Ex4 lowered the expression of ER stress markers through AMPK activation, as shown by **a**–**c** RT-PCR and **d**, **e** Western blotting. **f** Ex4 upregulated ERO1α expression through AMPK activation in HUVECs. $^{*}P < 0.05$ vs the Ctl group; $^{\#}P < 0.05$ vs the Hcy group; $^{\Delta}P < 0.05$ vs the Ex4 + Hcy group. $n = 5$ per group. **g**, **h** Chronic Ex4 treatment suppressed ER stress in aortae from the mice with diet-induced HHcy. **i** Chronic Ex4 injection elevated ERO1α expression in mouse aortae. $^{*}P < 0.05$ vs the Ctl group; $^{\#}P < 0.05$ vs the HMLF diet group. $n = 6$ per group· CC compound C, DHE dihydroethidium, Ex4 exendin-4, Ex9-39 exendin9-39, Hcy homocysteine, Tm tunicamycin, TUDCA tauroursodeoxycholic acid. The data are presented as the mean ± SEM.

not reciprocally activate AMPK. This is consistent with other previous studies showing that AMPK activation is upstream of the protein folding machinery in limiting ER stress in nonvascular tissues [34, 35]. A recent study reported that AMPK activation induces the expression of another ER chaperone, ORP150, in human bronchial cells to protect against ER stress and apoptosis [34]. Importantly, AMPK activation favors the generation of ATP, the cellular currency generally needed by certain ER chaperones such as BiP [35]. However, the detailed mechanism of how AMPK upregulates ER chaperones, such as ERO1α and ORP150, requires further investigation.

In the present study, knockdown of ERO1α did not completely abolish the ROS-lowering effects of exendin-4, indicating that GLP-1 analogs suppress oxidative stress through multiple mechanisms. These mechanisms are not limited to the AMPK/eNOS and AMPK/ERO1α pathways. In the functional assay, we showed that preincubation of exendin-4 and Met both rescued

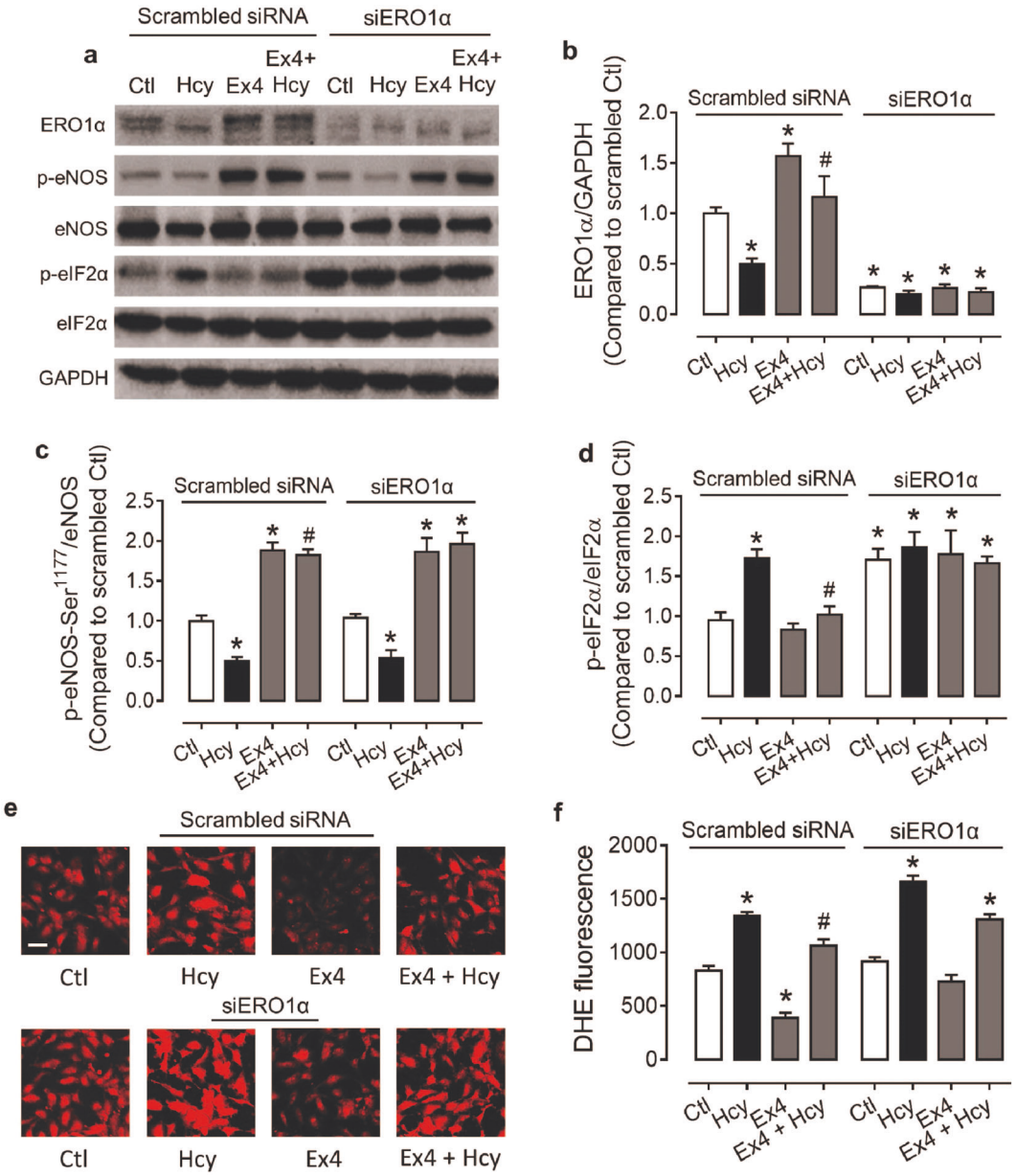

Fig. 7 siRNA-mediated ERO1α knockdown in HUVECs. a–d ERO1α knockdown increased ER stress but did not affect eNOS phosphorylation in HUVECs. **e**, **f** ERO1α knockdown attenuated the ROS-lowering effects of Ex4 in HUVECs (DHE staining, x200). $^{*}P < 0.05$ vs the scrambled Ctl group; $^{\#}P < 0.05$ vs the scrambled Hcy group. $n = 6$ per group. Ex4 exendin-4, Hcy homocysteine. The data are presented as the mean ± SEM.

EDRs against Hcy-induced endothelial dysfunction. We previously demonstrated that Met, a known AMPK activator, attenuates ER stress via the AMPK/PPARδ cascade to improve endothelial function in diabetic mice [18]. Another study also suggested that exendin-4 and the DPP4 inhibitor sitagliptin suppress oxidative stress through AMPK/UCP2-dependent mechanisms in endothelial cells in spontaneously hypertensive rats [29]. Therefore, it is reasonable to suggest that exendin-4, another AMPK activator, lowers oxidative stress via several targets, probably depending on the type(s) of pathological inducers.

Although the present study extends the vascular benefit of the GLP-1 analog exendin-4 beyond hypertension and diabetes, we are aware of some limitations. For example, the mechanism of AMPK-induced ERO1α upregulation by GLP-1 receptor activation warrants further investigation. In addition, we cannot rule out the contributions of other factors, albeit to a lesser degree, to the in vivo vasoprotective effect of exendin-4 in mice with diet-induced HHcy.

In conclusion, the present study provides new evidence that GLP-1 analogs induce AMPK activation to upregulate the ER chaperone ERO1α; the latter effectively inhibits ER stress in endothelial cells as the main mechanism for the exendin-4-induced preservation of endothelial function both in vitro and in vivo against HHcy (Fig. 9). These results indicate that GLP-1 analogs produce pleotropic effects directly against vascular dysfunction beyond their originally intended effects on glycemic control. Targeting ER stress may represent another useful and

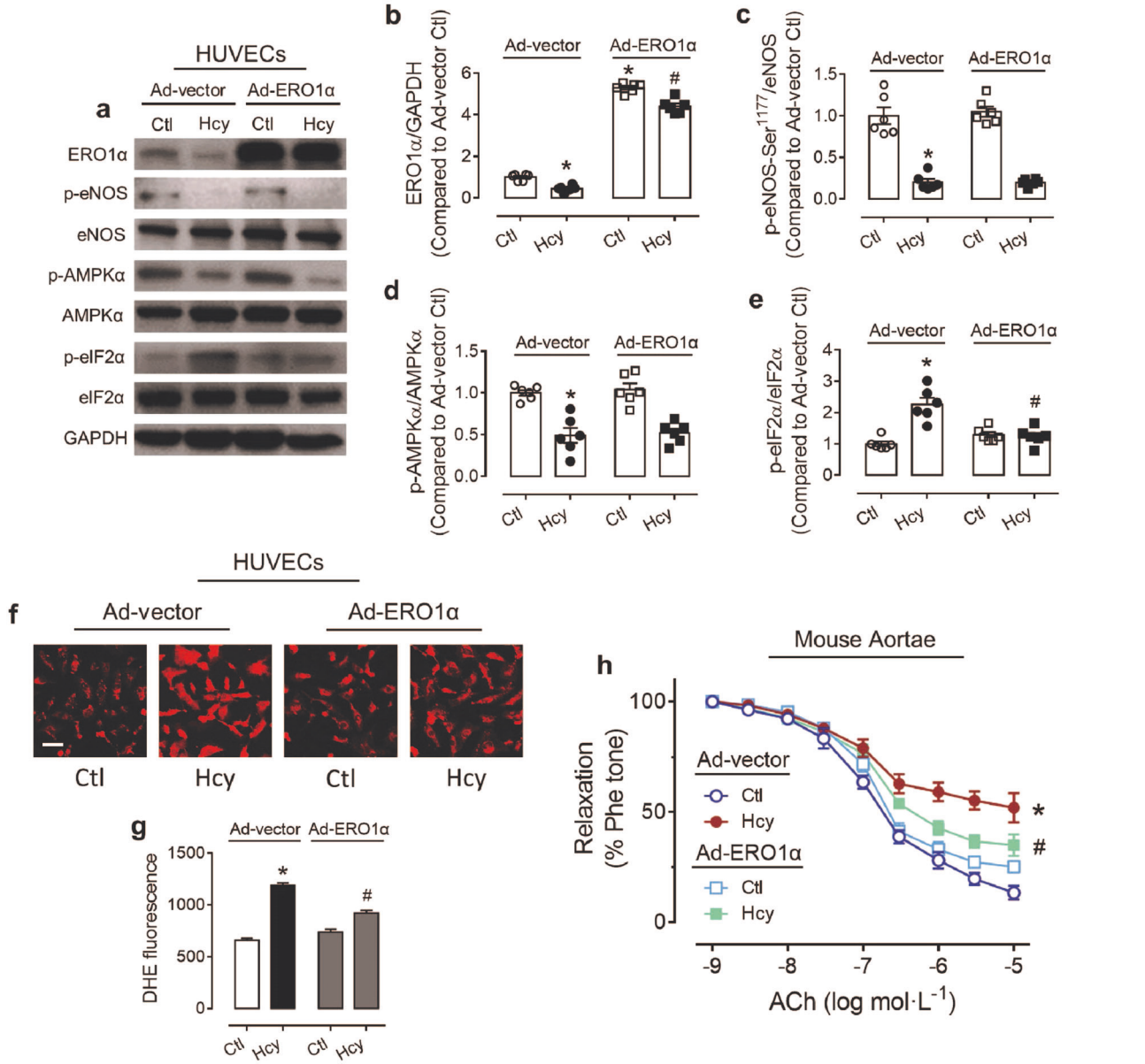

Fig. 8 ERO1α overexpression in HUVECs and mouse aortae. a–d ERO1α overexpression in HUVECs did not affect the phosphorylation of AMPK and eNOS. **a**, **e** ERO1α overexpression protected HUVECs against HHcy-induced ER stress in HUVECs. **f**, **g** ERO1α overexpression reversed HHcy-triggered oxidative stress in HUVECs (DHE staining, x200). **h** ERO1α overexpression improved endothelial function in HHcy-incubated mouse aortae. $^{*}P < 0.05$ vs the vector Ctl group; $^{\#}P < 0.05$ vs the vector Hcy group. $n = 6$ per group. Hcy homocysteine. The data are presented as the mean ± SEM.

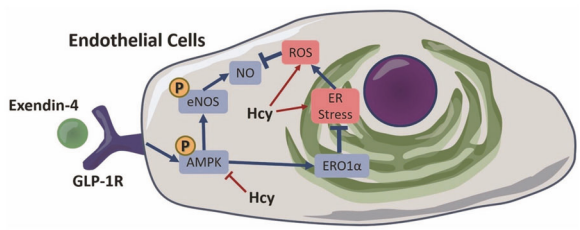

Fig. 9 The endothelial benefits mediated by exendin-4. By binding to GLP-1R in endothelial cells, exendin-4 activates the AMPK/eNOS axis to improve endothelial function. However, AMPK activation upregulates the expression of the ER chaperone ERO1α, which suppresses ER stress and hence ER stress-induced oxidative stress to improve endothelial function.

effective strategy for the prevention and treatment of endothelial dysfunction in cardiometabolic diseases.

ACKNOWLEDGEMENTS

This work was supported by Health and Medical Research Fund [Grant numbers 05162906 and 05161746], Early Career Scheme [Grant number 24122318], the National Natural Science Foundation of China [Grant numbers 91739103 and 91939302], and Hong Kong Research Grants Council [Grant numbers 14112919 and C4024-16W].

AUTHOR CONTRIBUTIONS

CKC designed the study, performed experiments, analyzed the data, and wrote the manuscript. CWL and JYL performed some of the experiments. WCsC, CFN, and RCWM were involved in regular discussion and revised the manuscript. YH and XYT

designed the study, analyzed the data, wrote the manuscript, and provided grant support.

ADDITIONAL INFORMATION

The online version of this article (https://doi.org/10.1038/s41401-020-00589-x) contains supplementary material, which is available to authorized users.

Competing interests: The authors declare no competing interests.

REFERENCES

1. Ganguly P, Alam SF. Role of homocysteine in the development of cardiovascular disease. Nutr J. 2015;14:6.
2. Shenoy V, Mehendale V, Prabhu K, Shetty R, Rao P. Correlation of serum homocysteine levels with the severity of coronary artery disease. Indian J Clin Biochem. 2014;29:339–44.
3. Hoogeveen EK, Kostense PJ, Jakobs C, Dekker JM, Nijpels G, Heine RJ, et al. Hyperhomocysteinemia increases risk of death, especially in type 2 diabetes. Circulation. 2000;101:1506–11.
4. Cheng Z, Yang X, Wang H. Hyperhomocysteinemia and endothelial dysfunction. Curr Hypertens Rev. 2009;5:158–65.
5. Xu J, Zou MH. Molecular insights and therapeutic targets for diabetic endothelial dysfunction. Circulation. 2009;120:1266–86.
6. Looker HC, Fagot-Campagna A, Gunter EW, Pfeiffer CM, Sievers ML, Bennett PH, et al. Homocysteine and vitamin B12 concentrations and mortality rates in type 2 diabetes. Diabetes Metab Res Rev. 2007;23:193–201.
7. Bhatia P, Gupta S, Sharma S. Homocysteine excess and vascular endothelium dysfunction: delineating the pathobiological mechanisms. Int J Pharmacol. 2014;10:200–12.
8. Liu L, Liu J, Huang Y. Protective effects of glucagon-like peptide 1 on endothelial function in hypertension. J Cardiovasc Pharmacol. 2015;65:399–405.
9. Jakubowski H. Homocysteine modification in protein structure/function and human disease. Physiol Rev. 2019;99:555–604.
10. Ji C, Kaplowitz N. Hyperhomocysteinemia, endoplasmic reticulum stress, and alcoholic liver injury. World J Gastroenterol. 2004;10:1699–708.
11. Lenna S, Han R, Trojanowska M. Endoplasmic reticulum stress and endothelial dysfunction. IUBMB Life. 2014;66:530–7.
12. Nadkarni P, Chepurny OG, Holz GG. Regulation of glucose homeostasis by GLP-1. Prog Mol Biol Transl Sci. 2014;121:23–65.
13. Li Y, Li X, Zheng X, Tang L, Xu W, Gong M. Disulfide bond prolongs the half-life of therapeutic peptide-GLP-1. Peptides. 2011;32:1400–7.
14. Garber AJ. Long-acting glucagon-like peptide 1 receptor agonists: a review of their efficacy and tolerability. Diabetes Care. 2011;34:S279–84.
15. Liu L, Liu J, Wong WT, Tian XY, Lau CW, Wang YX, et al. Dipeptidyl peptidase 4 inhibitor sitagliptin protects endothelial function in hypertension through a glucagon–like peptide 1–dependent mechanism. Hypertension. 2012;60:833–41.
16. Oeseburg H, deBoer RA, Buikema H, van derHarst P, vanGilst WH, Silljé HHW. Glucagon-like peptide 1 prevents reactive oxygen species–induced endothelial cell senescence through the activation of protein kinase A. Arterioscler Thromb Vasc Biol. 2010;30:1407–14.
17. Bretón-Romero R, Weisbrod RM, Feng B, Holbrook M, Ko D, Stathos MM, et al. Liraglutide treatment reduces endothelial endoplasmic reticulum stress and insulin resistance in patients with diabetes mellitus. J Am Heart Assoc. 2018;7:e009379.
18. Cheang WS, Tian XY, Wong WT, Lau CW, Lee SST, Chen ZY, et al. Metformin protects endothelial function in diet-induced obese mice by inhibition of endoplasmic reticulum stress through 5′ adenosine monophosphate–activated protein kinase–peroxisome proliferator–activated receptor δ pathway. Arterioscler Thromb Vasc Biol. 2014;34:830–6.
19. Cheang WS, Wong WT, Zhao L, Xu J, Wang L, Lau CW, et al. PPARδ is required for exercise to attenuate endoplasmic reticulum stress and endothelial dysfunction in diabetic mice. Diabetes. 2017;66:519–28.
20. Cunha DA, Ladrière L, Ortis F, Igoillo-Esteve M, Gurzov EN, Lupi R, et al. Glucagon-like peptide-1 agonists protect pancreatic beta-cells from lipotoxic endoplasmic reticulum stress through upregulation of BiP and JunB. Diabetes. 2009;58:2851–62.
21. Kilkenny C, Browne W, Cuthilll C, Emerson M, Altman DG. NC3Rs Reporting Guidelines Working Group. Animal research: reporting in vivo experiments: the ARRIVE guidelines. Br J Pharmacol. 2010;160:1577–9.
22. Wong WT, Tian XY, Xu A, Yu J, Lau CW, Hoo RLC, et al. Adiponectin is required for PPARγ-mediated improvement of endothelial function in diabetic mice. Cell Metab. 2011;14:104–15.
23. Wong SL, Lau CW, Wong WT, Xu A, Au CL, Ng CF, et al. Pivotal role of protein kinase Cδ in angiotensin II-induced endothelial cyclooxygenase-2 expression: a link to vascular inflammation. Arterioscler Thromb Vasc Biol. 2011;31:1169–76.
24. Gou L, Zhao L, Song W, Wang L, Liu J, Zhang H, et al. Inhibition of miR-92a suppresses oxidative stress and improves endothelial function by upregulating heme oxygenase-1 in db/db Mice. Antioxid Redox Signal. 2018;28:358–70.
25. Ling WC, Liu J, Lau CW, Murugan DD, Mustafa MR, Huang Y. Treatment with salvianolic acid B restores endothelial function in angiotensin II-induced hypertensive mice. Biochem Pharmacol. 2017;136:76–85.
26. Tyagi N, Sedoris KC, Steed M, Ovechkin AV, Moshal KS, Tyagi SC. Mechanisms of homocysteine-induced oxidative stress. Am J Physiol Circ Physiol. 2005;289:H2649–56.
27. Wei R, Ma S, Wang C, Ke J, Yang J, Li W, et al. Exenatide exerts direct protective effects on endothelial cells through the AMPK/Akt/eNOS pathway in a GLP-1 receptor-dependent manner. Am J Physiol Metab. 2016;310:E947–57.
28. Cheng CK, Bakar HA, Gollasch M, Huang Y. Perivascular adipose tissue: the sixth man of the cardiovascular system. Cardiovasc Drugs Ther. 2018;32:481–502.
29. Liu L, Liu J, Tian XY, Wong WT, Lau CW, Xu A, et al. Uncoupling protein-2 mediates DPP-4 inhibitor-induced restoration of endothelial function in hypertension through reducing oxidative stress. Antioxid Redox Signal. 2014;21:1571–81.
30. Zito E. ERO1: a protein disulfide oxidase and H2O2 producer. Free Radic Biol Med. 2015;83:299–304.
31. Feldman DE, Chauhan V, Koong AC. The unfolded protein response: a novel component of the hypoxic stress response in tumors. Mol Cancer Res. 2005;3:597–605.
32. Hogg PJ. Disulfide bonds as switches for protein function. Trends Biochem Sci. 2003;28:210–4.
33. Wright J, Birk J, Haataja L, Liu M, Ramming T, Weiss MA, et al. Endoplasmic reticulum oxidoreductin-1α improves folding and secretion of mutant proinsulin and limits mutant proinsulin-induced endoplasmic reticulum stress. J Biol Chem. 2013;288:31010–8.
34. Liu JQ, Zhang L, Yao J, Yao S, Yuan T. AMPK alleviates endoplasmic reticulum stress by inducing the ER-chaperone ORP150 via FOXO1 to protect human bronchial cells from apoptosis. Biochem Biophys Res Commun. 2018;497:564–70.
35. Pobre KFR, Poet GJ, Hendershot LM. The endoplasmic reticulum (ER) chaperone BiP is a master regulator of ER functions: getting by with a little help from ERdj friends. J Biol Chem. 2019;294:2098–108.